

# Numerical Analysis of Time Required for Destratification in Warehouses

Michael D. POLANDER<sup>1</sup>, Elsa D. HARDER<sup>1</sup>, Joseph F. JUNKER<sup>1</sup>, Brian M. FRONK<sup>1\*</sup>

<sup>1</sup>School of Mechanical, Industrial and Manufacturing Engineering  
Oregon State University  
Corvallis, OR, United States  
541-737-3952, brian.fronk@oregonstate.edu

\* Corresponding Author

## ABSTRACT

A large percentage of energy in buildings is consumed to for heating, cooling, and ventilation to maintain the indoor environments preferred for human comfort, and the storage of goods. One way to reduce energy costs for indoor enclosures is through the manipulation of thermal stratification. In heating, removing the stratification phenomena has been linked to savings due to the reduction in driving temperature difference at the ceiling. The primary method of destratification is the utilization of ceiling fans, which have a parasitic load that offsets energy savings.

A solution to eliminate the reliance on grid power is the use of solar photovoltaic powered fans that are not grid-tied. However, there is less solar resource available during the heating seasons when destratification is needed most. Thus, the objective of this study was to estimate the minimum required fan duty cycle to maintain a destratified temperature profile using a numerical analysis. The simulation assessed the time required to maintain a destratified environment based on inputs such as fan rated flow rate, spacing, and warehouse size. To establish the quality of the numerical analysis, two experiments were created to observe the impact of destratification. One experiment was located at a large distribution center, the other was a small classroom. The data collected from these experiments was be compared to the models developed to validate the findings. It was found that a destratification fan could maintain a destratified environment by operating for approximately 35% of a given time period.

## 1. INTRODUCTION

Within the residential and commercial sector in the United States, 25% of all energy usage is for space heating, primarily via natural gas. This energy usage represents \$40 billion in expenditures to maintain interior environmental conditions (EIA 2017). There is therefore an interest in reducing the energy required to heat large spaces. One method to potentially reduce energy costs for indoor enclosures is through the manipulation of thermal stratification. Warehouses are of interest as they represent large, relatively open enclosures with high ceilings and a corresponding high cost of heating.

Thermal stratification exists when there is a temperature gradient within a medium of interest. Within an unheated warehouse, stratification is most significant during the cooling season. During the heating season, there is little to no stratification (Porrás-Amores *et al.* 2014). Warmer air that is driven to the ceiling loses energy through the roof, dampening any stratification effect. When heating to the warehouse is added a noticeable stratification profile will develop. The temperature profiles are non-linear and have three main components: a lower cooler region with low relative stratification, an upper warmer region also with a low amount of stratification, and a region of very high stratification separating the two (Bouzinaoui *et al.* 2005).

For heating purposes, having a stratification profile present causes energy losses. As the warmer air collects at the ceiling, there is a considerable increase in the amount of energy required to maintain the occupied regions of the environment at comfortable conditions. To remove this stratification profile, mixing of the air, commonly referred to as destratification, is performed by the implementation of fans located at ceiling height. These fans force the warmer air located at the ceiling downward, mixing it with the cooler air below and bringing the environment to a uniform

temperature (Armstrong *et al.* 2009). Figure 1 is a simplified illustration of the pre- and post-mixed stratification profiles.

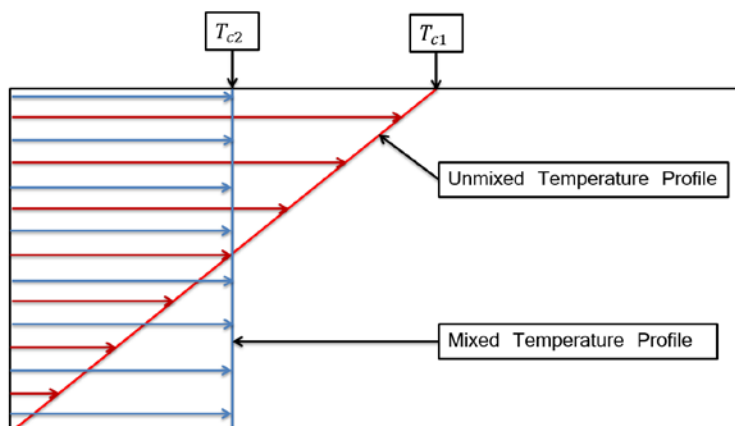


**Figure 1:** Destratification Savings Illustration

The primary savings attained through destratification are related to the decreased ceiling temperature. As the warehouse environment transitions from an unmixed to a mixed temperature profile, a temperature increase is seen for the lower half, and a temperature decrease is seen for the upper half, and the area of the two shapes is equivalent. The heat lost through the walls is unchanged, as the average temperature difference between the wall surface and ambient is not significantly impacted by destratification, and no savings are attained as a result. The other component is the change of the temperature at the ceiling height. This change reduces the difference between the interior and outdoor ambient temperatures, reducing the amount of heat lost through the ceiling and resulting in energy savings (Aynsley 2005).

Armstrong *et al.* (2009) performed a study which determined the savings due to the installation of destratification fans. For an 8,600 m<sup>2</sup> warehouse, a ceiling temperature reduction of 4 °C and a floor temperature increase of 1.5 °C was attained. This resulted in an annual natural gas savings of \$6440, which is a 19.3% reduction in fuel consumption for the studies warehouse. The fans themselves had an annual operational cost of \$326, a 5% parasitic loss on fuels savings. While in the case of Armstrong *et al.* (2009) the parasitic losses on destratification were much less than the gross energy savings, there are cases in which the cost of fan operation is large enough to negate the fuel savings Hughes (2006).

To gain the advantage of destratification without the parasitic power costs of a grid powered fan, solar photovoltaic powered fans that are not grid tied could be implemented. These devices could be applied to warehouse retrofits without the need for expensive electrical work, permitting and with zero incremental energy cost. However, there is a concern that the solar powered fans are most needed when the least solar power is available during the short winter days.

Thus, the objective of this study is to use experiments and simulation to understand the destratification process in warehouses. The results will be used to provide an estimate of the required run time for destratification fans to provide an energy savings effect for a given warehouse size, fan capacity, and ambient conditions. To determine a fan duty time, two models were developed. One model predicts mixing behavior, calculating the time required to achieve destratification. The other model calculates the time for the building to cool sufficiently that heaters need to be activated. The combination of these two models can be used to optimize control strategies of either solar or grid powered fans, and help designers size battery backup for solar powered fans so that minimum run times can be achieved. In parallel to the computational effort, experiments are conducted in a warehouse and smaller school room environment to measure stratification profiles with and without destratification fans operating. The models are compared to experimental data, collected by this study, for validation.

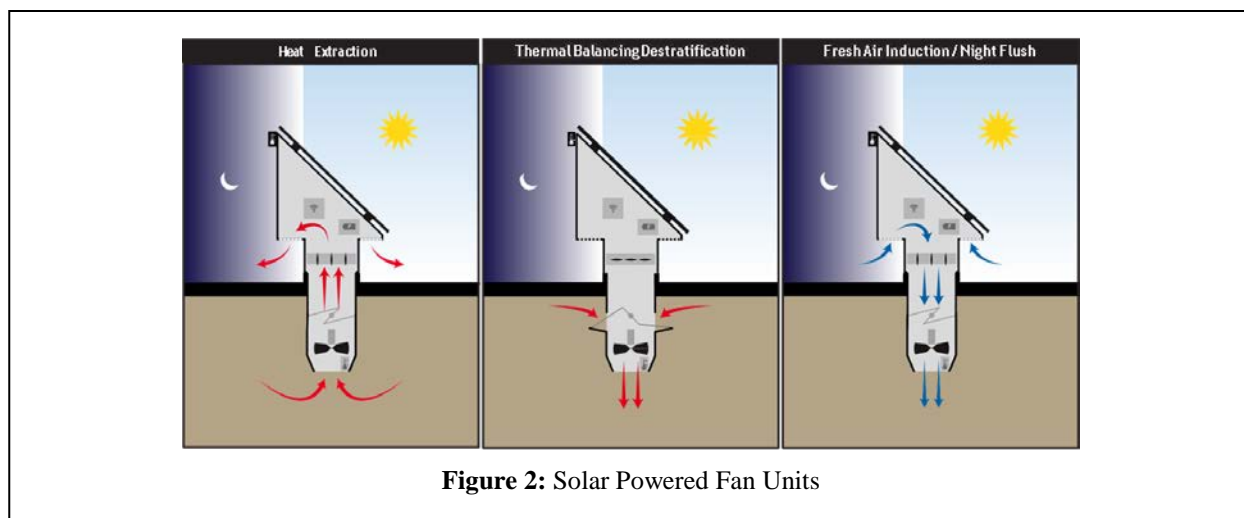


**Figure 2:** Solar Powered Fan Units

## 2. EXPERIMENT SETUP AND RESULTS

De-stratification experiments were conducted in two different building types and locations. The first was a 1.5 million square foot warehouse with seven fans installed in a dedicated experimental zone, while the second was a single school room with one solar drive unit installed. Within the warehouse, temperature data were obtained using a wireless sensor network at locations throughout the warehouse. For each location, data were collected at heights between 2.1 m and 9.8 m. The sensor network covered approximately 500,000 square feet of the warehouse, and included areas serviced by solar powered units (experimental zone), and areas well away from the solar powered units (control zone). The school room experiment was designed to collect temperature data at heights from 0.15 m to 2.1 m to characterize the induction cooling which the solar powered unit was designed to perform at that site. The solar powered devices utilized are shown in Figure 2.

These units are designed for three models of operation: induction cooling, exhaust cooling, and de-stratification. Induction cooling pulls air from the exterior and injects it into the interior. The exhaust cooling function operates when the external temperature is higher than the internal temperature. Removing the warmer air collected at the higher region of the room. Induction and exhaust have the goal of reducing the cooling load. The final setting is the de-stratification mode, which closes access to external air and operates to mix the interior air only. In the warehouse

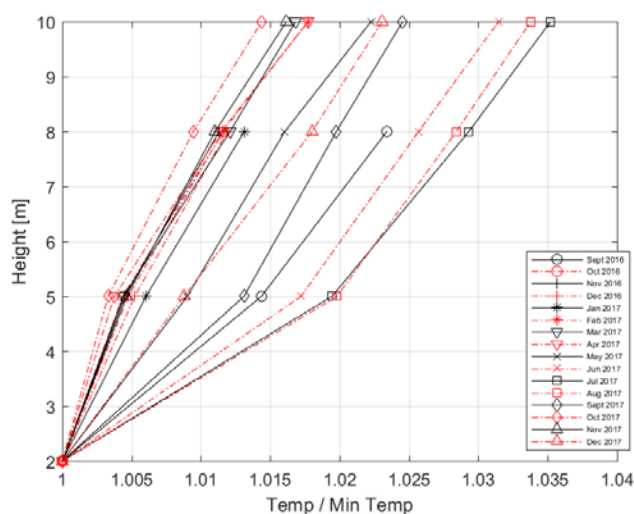


**Figure 3:** Month Averaged Temperature Profiles – Warehouse Experiment

each fan was had a nominal capacity of  $7.08 \text{ m}^3 \text{ s}^{-1}$  (15,000 CFM) and was primarily inspected in destratification mode. The fan installed in the schoolroom was designed for a nominal capacity of  $0.47 \text{ m}^3 \text{ s}^{-1}$  (1,000 CFM) and only had the ability to operate in induction cooling mode.

Figure 3 shows the normalized, monthly average temperatures for a central location within the experimental zone warehouse. When heating a warehouse, it is expected that a stratification profile will be apparent during all seasons. While stratification did exist during cooling months, it was reduced significantly during heating months, with average maximum temperature differences ranging from 0.2 to  $0.5^\circ\text{C}$ .

This data showed clearly that the temperature profiles behaved similarly to that of an unheated warehouse (Porras-Amores *et al.* 2014). The under heated scenario was further confirmed by the observation that the direct fired makeup air units operated nearly continuously during the heating months, suggesting that the thermostats are never satisfied. Thus, while the warehouse provided useful data for other aspects of this study, it was not expected to show significant benefits from destratification. This prompted the creation of a second experimental site, the school room. This site was only operated for 6 weekend periods in November and December, as the experiment addition came later in the study. With the schoolroom a heater was set to operate and develop a stratification profile. After the profile was developed, the solar powered fan unit was enabled in induction cooling mode. The resulting temperature profile for a 12-hour period is shown in Figure 4. This data is used to validate the predicative capability of the warehouse model.

### 3. MODEL DEVELOPMENT

#### 3.1 Model Setup

The goal of the modeling portion of this study is to predict the mixing and cooling behavior of air in a large-scale warehouse using a 3D computational fluid dynamic simulation. The model will produce estimates of required time for destratification for a given initial stratification profile and fan volumetric flow rate. It will also provide an estimate for how long the destratified profile will remain once fans have been turned off. Combined, this information will enable estimates of required destratification fan run time. ANSYS CFX and ANSYS ICEM CFD were utilized to develop and solve the models. The turbulence model employed was the standard  $k$ - $\epsilon$ .

The model has been designed to predict performance over a range of possible geometric parameters representative of warehouses. This expands the studies investigation to warehouses of different heights and for different destratification capabilities, and makes the results of the study applicable for more than just the experimental case.

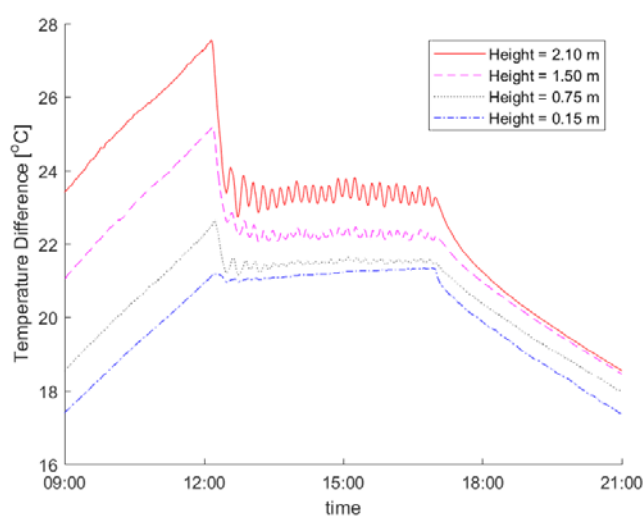


**Figure 4:** Temperature vs Time at discreet heights

The model domain contains nine inlets representing fans, as the modeling package used did not have the capability to model a fan directly. Each inlet supplies air at specified flow rate (representing different fans) at the ceiling temperature. The inlets were arranged so that fan-to-fan and fan-to-wall interactions could both be observed. As the model is designed with inlets, pressurization of the model needs to be accounted for. With destratification, no pressure build-up should occur as it would operate in a closed system, assuming doors and windows remain closed. Therefore, outlets need to be included in the model to ensure that a pressure buildup does not occur.

When deciding upon a geometry, the model needed to be small enough to run in a reasonable time frame, while also being large enough to capture the fans interactions with each other and the walls. It was decided that a geometry with nine fans in a  $3 \times 3$  grid would best satisfy this requirement. The model geometry is shown in Figure 6. The nine blue spots on the top of the box are inlets which represent fans. The fans represented will be the  $7.08 \text{ m}^3 \text{ s}^{-1}$  and  $1.18 \text{ m}^3 \text{ s}^{-1}$  solar powered fan units. The inlet geometry is determined by which flow rate will be set at the boundary. The protrusions on the side of the box are outlets provided to ensure that the model roughly maintains the expected atmospheric pressure. Model that were run, and their parameters, are shown in Table 1.

### 3.2 Meshing

Three different evaluations were performed to ensure mesh and timestep quality. A grid independence study, an evaluation of  $y^+$  values, and a time independence study. The evaluation of  $y^+$  values was performed for every mesh

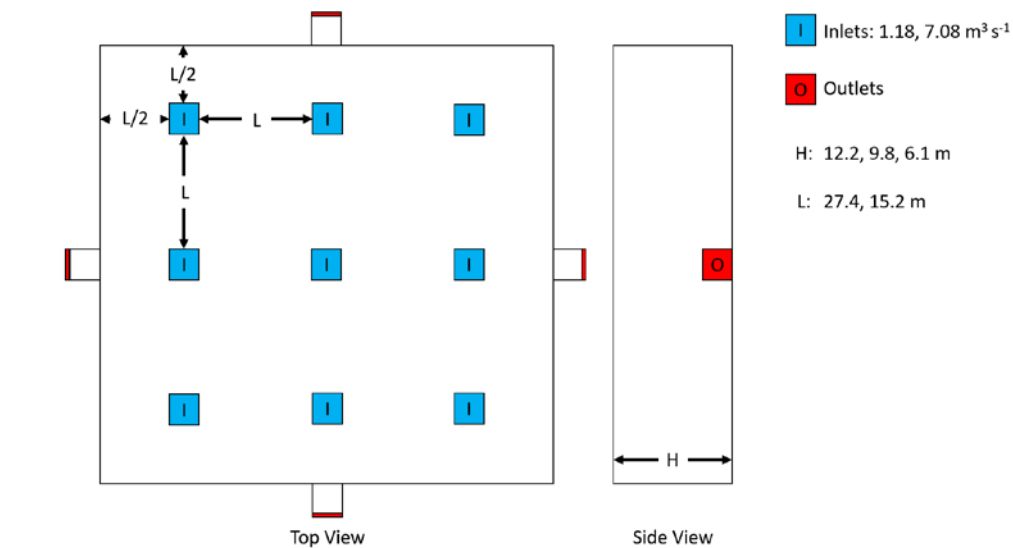


Figure 6: Model Geometry

Table 1: Models Run

Fan Volumetric Flow Rate	Ceiling Height	Fan Spacing	Exterior Temperature	External Heat Transfer Coefficient ASHRAE (2017)
$7.08 \text{ m}^3 \text{ s}^{-1}$	12.2 m	27.4 m	$-15^\circ\text{C}$	$0.3 \text{ W m}^{-2} \text{ K}^{-1}$
$7.08 \text{ m}^3 \text{ s}^{-1}$	9.8 m	27.4 m	$-15^\circ\text{C}$	$0.3 \text{ W m}^{-2} \text{ K}^{-1}$
$1.18 \text{ m}^3 \text{ s}^{-1}$	9.8 m	15.2 m	$-15^\circ\text{C}$	$0.3 \text{ W m}^{-2} \text{ K}^{-1}$
$1.18 \text{ m}^3 \text{ s}^{-1}$	6.1 m	15.2 m	$-15^\circ\text{C}$	$0.3 \text{ W m}^{-2} \text{ K}^{-1}$
N/A	6.1 m	N/A	$-15^\circ\text{C}$	$0.3 \text{ W m}^{-2} \text{ K}^{-1}$

created. Prior to running the full simulation, each mesh was run to steady state with energy solving disabled. The  $y^+$  were then inspected to ensure that they were between 30 and 500, which is within the log law region of the universal velocity profile and is the value expected by the standard  $k$ - $\epsilon$  model (Versteeg and Malalasekera 1995). The grid independence study was performed by first doing an initial run, then increasing the number of cells per fluid block and performing another run. The results of each run are then compared and if the difference is small, the previous grid size is appropriately fine for the evaluated geometry. If the difference is large, the process is repeated until there is no longer a significant difference in the results. In this study, the time required for temperature to converge to within  $0.25^\circ\text{C}$  was compared. As the geometries being evaluated are similar, only differing in scale, a single grid independence study was performed and the ratio of approximately 1 cell for 1 foot of physical distance was found to be an acceptable guideline for meshing each geometry. The time independence study was performed by determining the largest timestep possible while maintaining RMS residuals of  $1 \times 10^{-4}$  or less. This was found to be  $1 \times 10^{-5}$  seconds for initial time steps, growing by an order of magnitude until the timestep was equal to 0.5 seconds. The model was then able to run and maintain residuals of  $1 \times 10^{-4}$  or better.

### 3.3 Model Parameters

Two different types of models were run, one for mixing with the fans operational, and the other for cooling with the fans turned off. Most of the model parameters are identical, except that in the cooling model the inlets and outlets are removed. All parameters discussed apply to both models, with the exception of the removed boundary conditions. For the ceiling and walls of the simulated warehouse, the boundaries were set with a heat transfer coefficient of  $0.3 \text{ W m}^{-2} \text{ K}^{-1}$  and an external temperature of  $-15^\circ\text{C}$ . The heat transfer coefficient was selected based on data available in the ASHRAE Fundamentals Handbook (ASHRAE 2017). The average temperature for each state during winter months is also available in the ASHRAE handbook, the lowest average temperature was selected so that the most extreme cooling case would be studied and provide a more conservative estimate on the cooling rate. The floors were set to be adiabatic, no slip, walls. The inlets are set to be subsonic flow, as the fans are rated for relatively low velocity. For mass and momentum, the inlets are assigned a velocity which is derived from the solar powered fan rated flow capacity and the inlet area. Both of which are provided by the solar powered fan specification sheets NWREC (2017).

Outlets were defined as pressure openings. This is to allow flow at the outlet to vary as needed. Allowing the fluid to exit or enter through the outlets, as the pressure of the room dictates. This allows the room to maintain a relatively balanced pressure profile. The relative pressure of the inlet was set to 30 Pa. The turbulence intensity was set at the same value as the inlets. The opening temperature was set to  $-15^\circ\text{C}$  (ASHRAE 2017). Fluid properties were defined from the CFX library as air at  $25^\circ\text{C}$  and a reference pressure of 1 atmosphere. For initial conditions, all velocity directions are assumed to be at rest with a static pressure of 30 [Pa] relative to atmospheric pressure. The initial temperature profile was selected from a study by Aynsley (2005) and based on the heating method utilized by the warehouse Aynsley (2005). Within the model, the profile was defined using three linear equations increasing from  $15.6^\circ\text{C}$  at floor level to  $16.7^\circ\text{C}$  at nine tenths of the ceiling height, then to  $20^\circ\text{C}$  at halfway between ceiling height at the previous height, rising to  $21^\circ\text{C}$  at ceiling height. The temperature value remained the same for all geometries with only the ceiling height adjusting the profile. To capture the buoyant effects of the temperature gradient, buoyancy is enabled with gravity set to be  $-9.81 \text{ m s}^{-2}$  in the vertical direction ( $z$ ). The buoyancy reference temperature is set to as  $20^\circ\text{C}$ .

Models were run for a set number of time steps, then checked periodically to determine if mixing had completed. After a sufficient number of time steps, the temperature difference between the inlet jets will be less than  $0.25^\circ\text{C}$ . When this is observed, mixing is considered to be completed. The cooling model does not have as clear of a stopping point as the minimum allowable temperature is dependent on preference. Instead, it will be determined how long is required for the lowest elevation in the room to see a  $0.5^\circ\text{C}$  drop in temperature. With the results from mixing and cooling models, a duty cycle can be recommended for fans installed for the purpose of destratification.

## 4. RESULTS

### 4.1 Mixing Results

All mixing scenarios run had similar flow development, the model with  $1.18 \text{ m}^3 \text{ s}^{-1}$  inlets, 6.1 m ceiling height, and 15.2 m fan spacing will be used for illustration. The results from the second run listed in Table 1 will be used for

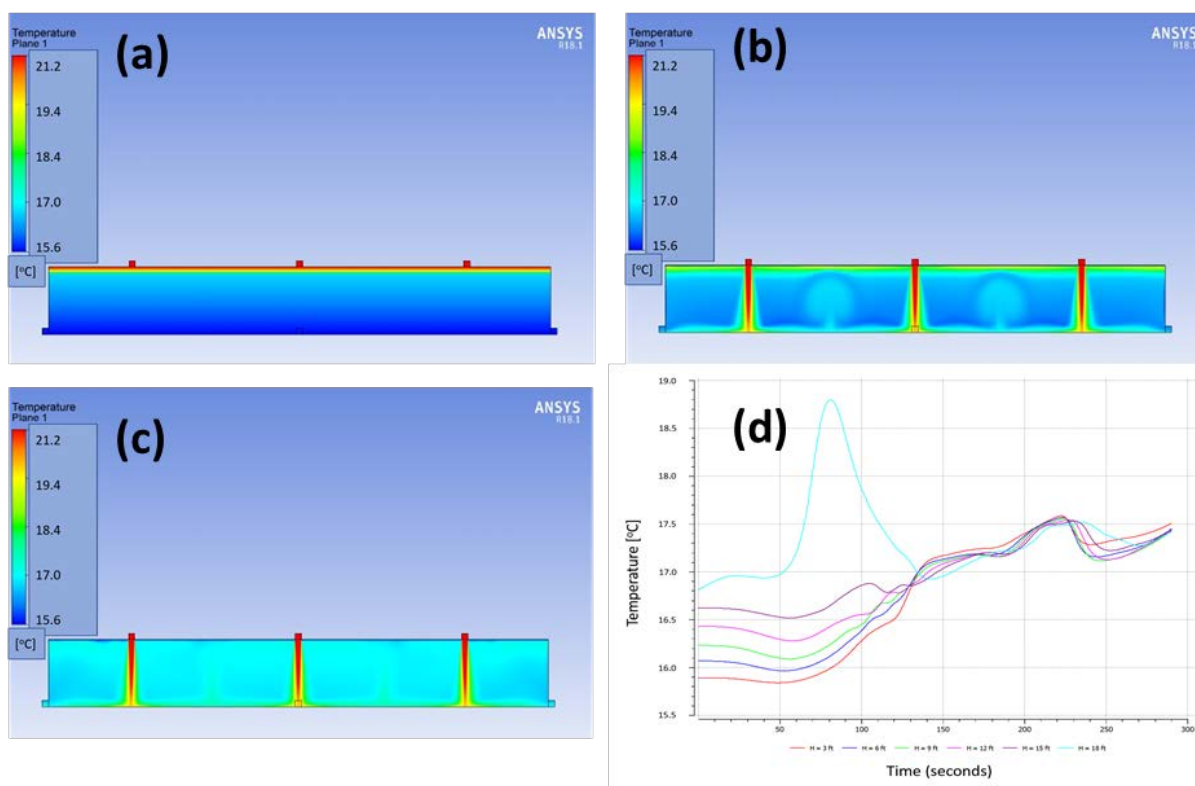


**Figure 7:** Mixing Results, (a) time = 0 seconds (b) time  $t = 68$  seconds (c) time = 148 second and (d) overall mixing results

**Table 2:** Model Results

Fan Volumetric Flow Rate	Ceiling Height	Fan Spacing	Exterior Temperature	External Heat Transfer Coefficient ASHRAE (2017)	Time to Completion
$7.08 \text{ m}^3 \text{ s}^{-1}$	12.2 m	27.4 m	$-15^\circ\text{C}$	$0.3 \text{ W m}^{-2} \text{ K}^{-1}$	162 s
$7.08 \text{ m}^3 \text{ s}^{-1}$	9.8 m	27.4 m	$-15^\circ\text{C}$	$0.3 \text{ W m}^{-2} \text{ K}^{-1}$	144 s
$1.18 \text{ m}^3 \text{ s}^{-1}$	9.8 m	15.2 m	$-15^\circ\text{C}$	$0.3 \text{ W m}^{-2} \text{ K}^{-1}$	N/A
$1.18 \text{ m}^3 \text{ s}^{-1}$	6.1 m	15.2 m	$-15^\circ\text{C}$	$0.3 \text{ W m}^{-2} \text{ K}^{-1}$	148

visualization purposes. Figure 7a shows the initial temperature profile of the simulation. Figure 7b shows a point midway between the initial temperature profile and the mixed profile. At this point the velocity profile has begun to entrain and move warmer air located at the ceiling down into the cooler air for mixing. In Figure 7c mixing has completed and a uniform temperature profile is observed in the regions between the warm inlet jets. Finally, to confirm that mixing had completed, monitors were placed in the model and when temperature converged sufficiently the run was considered complete. An example of monitors converging can be seen in Figure 7d. Results from all mixing models are shown in Table 2:

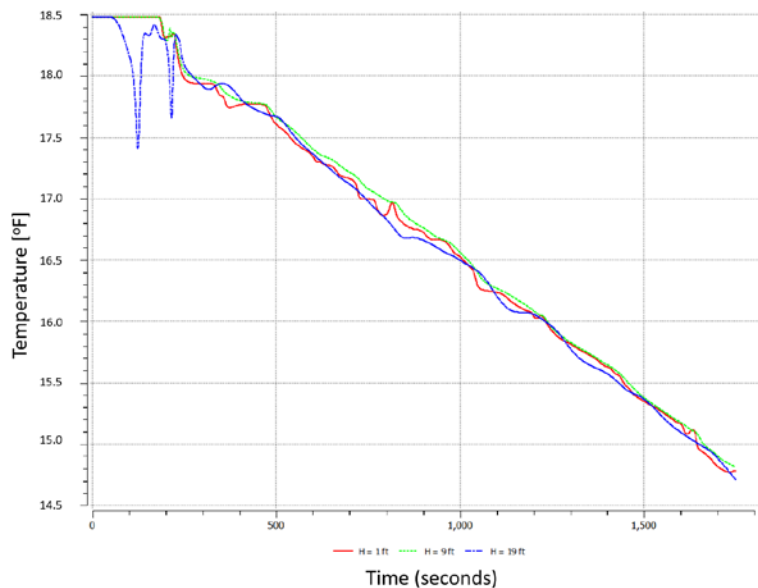
#### 4.2 Cooling Results

Figure 8 shows the temperature monitors within the cooling model for the duration of the run. For the first  $\sim 380$  seconds of cooling, the flow fields are developing and cooling is non-linear. After 380 seconds, cooling settles into a linear behavior which continues for the duration of the model. The requisite temperature drop is hit within the non-linear zone at time equal to 280 seconds.

### 4.3 Validation

To determine the quality of the simulations, a validation model was created of the school room experiment. All solver settings were kept identical to the mixing and cooling models. The model was run to an hour of simulation time and the results were compared to the data collected from the school room experiment, shown in Figure 9.

The initial model results show that the model is cooling much more quickly than experimentally observed. To understand why this might be occurring, the time axis of data collected from the school room was divided by a constant so that the temperature data concluded at the overlap point with the model temperature data, shown in Figure 10. With the current model setup, the model is cooling approximately 29 times faster than is reflected in reality at the highest measured point in the room. The 0.15 m elevation cools significantly faster than that. The sharp drop at the initial time steps for the 0.15 m height show that the air entering through the cooler inlet is having a



**Figure 8:** Cooling Results

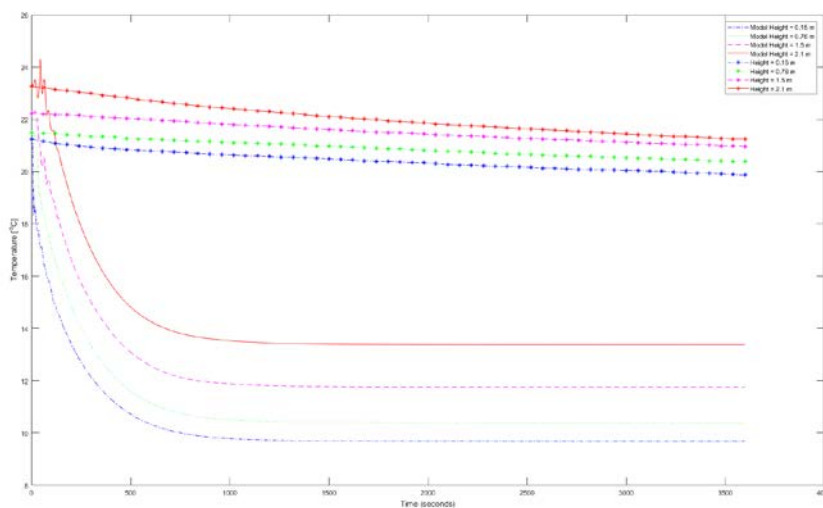


**Figure 9:** Model vs Actual Experimental Temperature

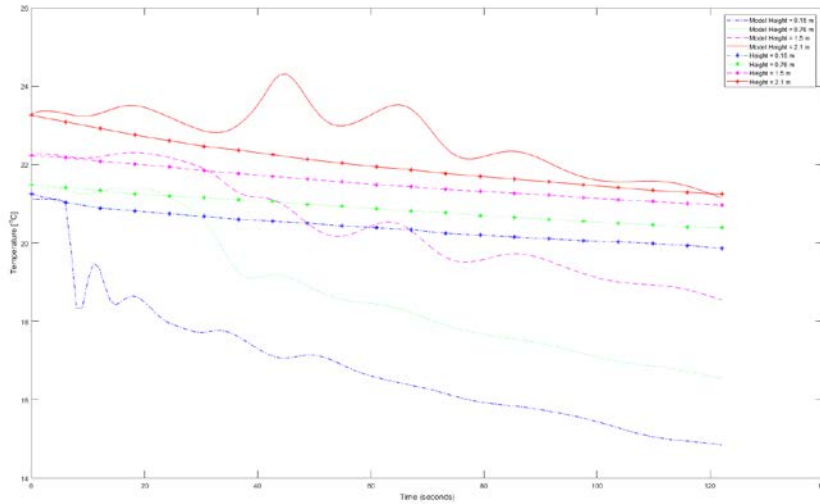


**Figure 10: Model vs Modified Experimental Temperature**

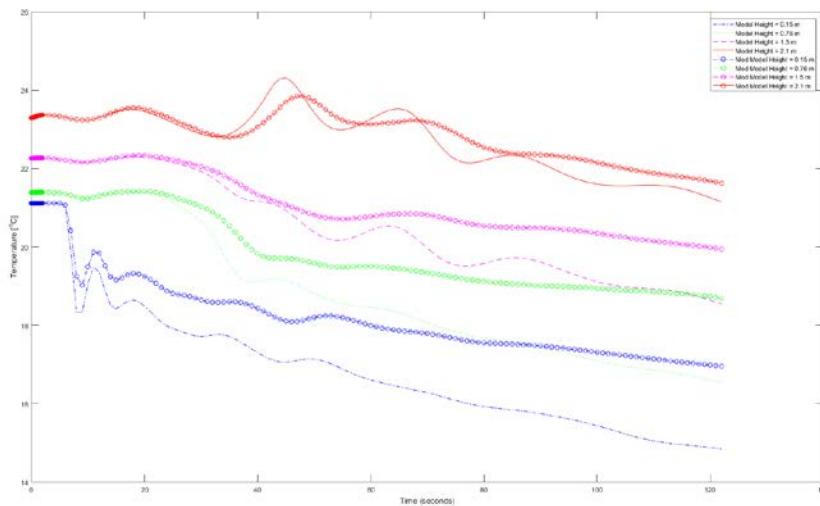


**Figure 11: Comparison of Model Data, with and without a Heated Floor**

much quicker impact than it should. This suggests that thermal mass has a very large part to play in the cooling profile shown by the collected data points. To verify this, another model was run with the floor temperature set at 26.7 °C. This value is artificially high to gauge the impact that changing it has on the models cooling profile. The new results were then compared to the previous model in Figure 11.

The modified experimental data has a linear slope of 0.023 and an average temperature difference of 1.7 °C. The initial model data had a slope of 0.063 and an average temperature difference of 2.8 °C. By adding a floor temperature, the slope of the model data is decreased to 0.043. Indicating the model more closely resembles experimental data. Additionally, the average temperature difference is reduced to 2.3 °C, which also more closely resembles to modified experimental data. This supports the conclusion that thermal mass has a significant role to play in cooling behavior and time. The model itself still cools much more rapidly than reality, but the profile declines in an expected way.

## 5. CONCLUSIONS

Results of the two models:

- Mixing requires 148 – 162 seconds depending on geometry.

- Cooling requires approximately 280 seconds.

Due to the lack of thermal mass present in the model, the mixing time is optimistic and that the cooling time is conservative. Thus, these results provide a qualitative approximation of required fan operation times, but more detailed investigation is required. While these values are not the exact times that would be required to perform mixing and cooling, the combination of the two models creates a ratio which can be utilized as a guideline for implementation of destratification systems. The finding of this study is that destratification fans nominally only need to operate for 35% of total operating time to maintain a destratified environment. This is shown in Equation (1):

$$\text{Operation Time} = \frac{\text{Fan run time}}{\text{Total time}} = \frac{148 \text{ seconds}}{148 \text{ seconds} + 280 \text{ seconds}} = 35\% \quad (1)$$

This duty cycle suggests that the solar powered destratification units may be able to perform destratification in colder regions if there is sufficient solar power and storage capacity for the units to operate and for 35% of the day cycle.

## ACKNOWLEDGMENTS

This material is based upon work supported by Oregon Built Environment and Sustainable Technologies Center (Oregon BEST) under Project Number CG-SOW-2016-OSU-NWREC. Technical support and operational assistance with solar powered ventilation by Mr. Jason Wright of Northwest Renewable Energy Corp. is gratefully acknowledged.

## REFERENCES

- Armstrong, M., Chihata, B., & MacDonald, R. (2009). Cold weather destratification energy savings of a warehousing facility. *ASHRAE Transactions*, 115(2), 513–518.
- ASHRAE. (2017) *ASHRAE Handbook - Fundamentals*. ASHRAE.
- Aynsley, R. (2005). Saving heating costs in warehouses. *ASHRAE Journal*, 47(12), 46–51.
- Bouzinaoui, A., Vallette, P., Lemoine, F., Raymond Fontaine, J., & Devienne. R., (2005). Experimental study of thermal stratification in ventilated confined spaces. *International Journal of Heat and Mass Transfer*, 48(19), 4121–4131.
- Hughes, J.C., (2006) Technology evaluation of thermal destratifiers and other ventilation technologies. In *American Industrial Hygiene Conference & Exposition, Chicago, Illinois (AIHce EXP)*. <https://www.aiha.org/aihce06/handouts/d1hughes.pdf>.
- NWREC. Northwest Renewable Energy Corp. Available at [http://www.nwrec.us/application/files/8015/0256/8559/Complete\\_Specs\\_v2.9.pdf](http://www.nwrec.us/application/files/8015/0256/8559/Complete_Specs_v2.9.pdf) Accessed (2017/19/12).
- Porras-Amores, C., Mazarron F.R., & Canas I. (2014). Study of the vertical distribution of air temperature in warehouses. *energies*, 7, 1193–1206.
- U.S Energy Information Administration (2017, May 19). *U.S. Energy Facts Explained*. Retrieved from [https://www.eia.gov/energyexplained/?page=us\\_energy\\_home](https://www.eia.gov/energyexplained/?page=us_energy_home)
- Versteeg, H.K., & Malalasekera, W., (1995). *An Introduction to Computational Fluid Dynamics: The Finite Volume Method*. Addison Wesley Longman Limited, Edinburgh Gate, Harlow, Essex CM20 2JE, England.